

PHYSICAL REVIEW C

NUCLEAR PHYSICS

THIRD SERIES, VOLUME 39, NUMBER 3

MARCH 1989

Fragmentation of high-spin particle-hole states in ^{26}Mg

R. E. Segel

*Northwestern University, Evanston, Illinois 60204**
and Argonne National Laboratory, Argonne, Illinois 60439

A. Amusa,[†] D. F. Geesaman, R. D. Lawson, and B. Zeidman
Argonne National Laboratory, Argonne, Illinois 60439

C. Olmer, A. D. Bacher, G. T. Emery, C. W. Glover, H. Nann, and W. P. Jones
Indiana University Cyclotron Facility, Bloomington, Indiana 47405

S. Y. van der Werf
Kernfysisch Versneller Instituut, Groningen, the Netherlands

R. A. Lindgren
University of Virginia, Charlottesville, Virginia 22901
(Received 31 October 1988)

The inelastic scattering of 134 MeV protons to 6^- states in ^{26}Mg has been studied. Five 6^- states were identified on the basis of their measured angular distributions and analyzing powers. By combining the results with those of companion electron scattering and (p,n) studies in ^{26}Mg and proton studies in ^{28}Si , it has been possible to extract isoscalar and isovector excitation amplitudes for each state.

I. INTRODUCTION

Systematic information is now being obtained from inelastic scattering and charge exchange reactions on the excitation of spin-flip degrees of freedom throughout the periodic table. Considerably more data is available on isovector spin-flip strength¹ since both charge exchange and inelastic scattering to $T_>$ states are pure isovector and magnetic electron scattering is nearly so. In contrast, it is only in self-conjugate nuclei that isoscalar strength can be measured without having to be separated from an interfering isovector amplitude. Inelastic proton and pion scattering reactions indicate that the quenching of spin-flip strength is even greater in the isoscalar than in the isovector mode,¹⁻⁴ but the systematics of this effect are not established.

Several theoretical explanations have been offered for the reduction in the spin-flip strength. These explanations include fragmentation of the single-particle strength,^{5,6} large two-particle, two-hole correlations due to the tensor force,⁷ mesonic renormalization of the spin current,⁸ and the explicit inclusion of $\Delta(1232)$ isobar-hole states.⁹ The last two mechanisms do not contribute significantly in isoscalar channels. One approach to separate these mechanisms is to study the inelastic transition strengths as a function of single-particle occupation probability and angular momentum. Data for neighboring nuclei exist only in the p shell and the (sd) shell, but in ^{12}C , ^{14}N , and ^{16}O substantial isospin mixing introduces

complications for the high-spin (4^-) states.¹⁰⁻¹² The deformed nuclei in the (sd) shell seem to be excellent candidates for these studies with several high-spin, 6^- , and low-spin, 1^+ , states known from previous experiments.^{2,3,13}

A major constraint in these studies is the lack of a suitable selective probe of the isoscalar spin-flip strength. In a $T=1$, $T_z=1$ nucleus like ^{26}Mg , one-particle one-hole excitations can form both $T=1$ and 2 states. While the excitation of the $T=2$ states must be pure isovector, $T=1$ states will be formed by a combination of isoscalar and isovector excitations. The present work reports the results of the scattering of 134-MeV polarized protons to populate 6^- states in ^{26}Mg . It is shown that these results, combined with data from dominantly isovector probes, (e,e') and (p,n) reactions,^{14,15} can be used to decompose the excitation of a given state into its separate isospin components. The data are analyzed in terms of experimental distributions measured for pure isospin transitions to 6^- states in ^{28}Si at the same incident energy. The isospin decomposed strengths are compared with previously published data on ^{24}Mg and ^{28}Si to study the variation of quenching as the s - d shell is filled.

II. EXPERIMENTAL RESULTS

Polarized protons from the Indiana University Cyclotron Facility were scattered by a 8.45-mg/cm^2 ^{26}Mg target, enriched to $>98.8\%$ ^{26}Mg , and analyzed by the quadrupole-dipole-dipole-multipole magnetic spectrom-

ter. The magnitude of the beam polarization was about 70%. The polarization was checked every few hours and did not vary significantly throughout the run. The direction of the polarization was reversed once a second.

Data were taken every 5° from 10° to 60° for states in the excitation range from 0 to 20 MeV. Four field settings of the spectrometer (each 9 MeV wide to allow considerable overlap) were required in order to cover this range. In addition, data were taken at 35° with a Si target where the yield to the ground state (0^+) and the 11.48 MeV $T=0$ and the 14.35 MeV $T=1$ 6^- states² were used to check the solid angle and energy calibration of the spectrometer. The energy resolution was approximately 80 keV full width at half maximum. A typical spectrum is shown in Fig. 1. Spectra were fit using the multipeak (roughly 20–40 peaks were simultaneously fit) spectrum fitting program AUTOFIT. The reference peak shape was taken from an isolated low-lying state. Consistent excitation energies were used for each angle and spin direction with the energy calibration determined by known low-lying ^{26}Mg and ^{28}Si states up to 14.35-MeV excitation energy. These multipeak fits on a smooth background describe the spectra well up to 13-MeV excitation, and angular distributions and analyzing powers were extracted for all states up to this excitation energy. Based on the angular distributions, 6^- states were identified at 9.18 ± 0.03 , 11.98 ± 0.03 , 12.49 ± 0.03 , and 12.85 ± 0.03 MeV, and 5^- levels were identified at 7.96 ± 0.03 and 8.62 ± 0.03 MeV excitation. Patterns for the characteristic shapes of the angular distributions were obtained from distorted-wave impulse approximation (DWIA) calculations (discussed in Sec. III) and experimental data for high-spin states¹⁶ in ^{24}Mg and ^{28}Si . Above 13 MeV, some of the discrete states appear to have widths greater than 80 keV, and all appear to lie on top of a significant continuum background. The strong state at 18.05 ± 0.05 MeV could also be clearly identified as a 6^- level. Other-

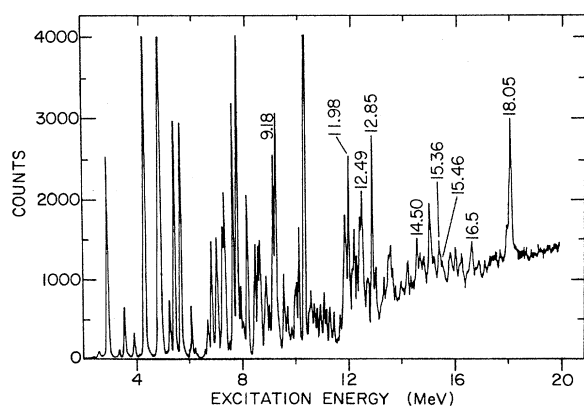


FIG. 1. Spectra at 45° of spin-up protons inelastically scattered by ^{26}Mg . Energies are given for the peaks corresponding to states believed to be 6^- . With the standard conventions for spin observables, and our geometry, a positive analyzing power corresponds to σ (spin up) $<$ σ (spin down). Since the analyzing powers of the 6^- states are positive at this angle, this spectrum deemphasizes the 6^- contributions to give a realistic “typical” spectrum.

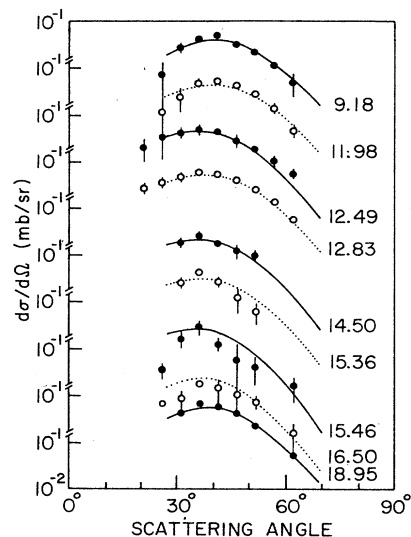


FIG. 2. Differential cross sections for the candidate 6^- states identified in this work or in Ref. 14. The lines represent the best fits to the (e, e') and (p, p') data for a 6^- state using proton amplitudes taken from ^{28}Si and the structure amplitudes of Table I.

wise, the only regions in the 13–20 MeV excitation energy range that were analyzed with multipeak fits were those where electron scattering angular distributions indicated possible 6^- states. Angular distributions were obtained for peaks corresponding to states seen in (e, e') at 14.50 ± 0.05 , 15.36 ± 0.05 , 15.46 ± 0.05 , and 16.50 ± 0.05 MeV. These states are discussed in more detail below. Due to the complexity of the spectra, other states of comparable 6^- strength could have been missed in the 13–20 MeV energy interval.

Based on its strong excitation in (e, e') (Ref. 14) and

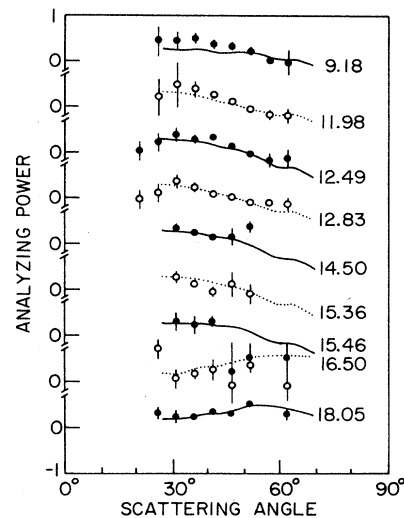


FIG. 3. Analyzing powers for the candidate 6^- states identified in this work or in Ref. 14. The lines are the analyzing powers predicted using the isospin amplitudes from the fits to the differential cross sections and the measured analyzing powers in ^{28}Si and the structure amplitudes of Table I.

systematics, the 18.05-MeV state is believed to be the lowest $T=2$, 6^- state. All the lower-energy states are assigned $T=1$. Differential cross sections for each of these states are shown in Fig. 2 and for analyzing powers are shown in Fig. 3. Also shown in Figs. 2 and 3 are the differential cross sections and analyzing powers that are obtained for each state using the isospin amplitudes that best fit the (p,p') and (e,e') data for a 6^- excitation. The procedures for obtaining the fitted curves are detailed below.

III. EXTRACTION OF ISOSPIN AMPLITUDES

If one describes the 0^+ ground state of ^{26}Mg and the 6^- states in terms of $(1d, 2s, 1f, 2p)$ wave functions, and inelastic scattering as a one-body transition operator, then only *one* single-particle matrix element can contribute to a 6^- excitation for each isospin. This immediately implies that the inelastic scattering cross sections for different probes are simply related. The (p,p') scattering cross section for exciting the i th 6^- state can be written for each spin state as

$$\left[\frac{d\sigma^p}{d\Omega} \right]^i = |Z_0^i M_0^p + Z_1^i M_1^p|^2, \quad (1)$$

where $M_{0(1)}^p$ are the complex isoscalar (isovector) transition amplitudes for pure single-particle excitation of a $d_{5/2}$ nucleon from an occupied subshell to an empty $f_{7/2}$ orbit and $Z_{0(1)}^i$ are nuclear structure amplitudes for these isoscalar (isovector) particle-hole excitations:

$$Z_T^i = \langle i, 6^-, T_f || [a_{7/2}^\dagger x a_{5/2}]_{J=6, T} || 0, 0^+, T=1 \rangle. \quad (2)$$

The experimental cross sections and analyzing powers are the usual sum and normalized difference of the cross sections for spin-up and spin-down protons. In a similar way, the electron scattering cross section to the i th 6^- state is

$$\left[\frac{d\sigma^e}{d\Omega} \right]^i = |Z_0^i M_0^e + Z_1^i M_1^e|^2, \quad (3)$$

where $M_{0(1)}^e$ are the transition amplitudes for $d_{5/2} \rightarrow f_{7/2}$ electron scattering. $M_{0(1)}^e$ are related by the expression

$$M_0^e = \frac{\mu_n + \mu_p}{\mu_n - \mu_p} M_1^e = -0.187 M_1^e, \quad (4)$$

where the free particle values of the neutron and proton magnetic moments have been used in the numerical estimate. The electron single-particle excitation amplitudes M^e are well known, subject to meson exchange corrections. If the proton amplitudes were equally well understood, then the three experimental observables ($d\sigma^e/d\Omega$, $d\sigma^p/d\Omega$, A^p) would determine the two nuclear structure amplitudes, Z_0 and Z_1 .

The (p,n) charge exchange reactions on the same target will populate mirror states in a purely isovector excitation. However, for a $T=1$ target such as ^{26}Mg , the (p,n) reaction can populate final states with isospin 0, 1, or 2. The $T=0$ states are not accessible in inelastic scattering reactions. In general, the isospin of the final state is not known, and so this may cause confusion in relating the appropriate analog states between ^{26}Al and

^{26}Mg . For a particular analog state

$$\left[\frac{d\sigma^{(p,n)}}{d\Omega} \right]^i = |Z_1^i M_1^{(p,n)}|^2. \quad (5)$$

Given the dominant isovector selectivity of the (e,e') and (p,n) reactions, they provide similar information. The (p,n) reaction is pure isovector, while the reaction mechanism is much better understood in (e,e') . Either one can be combined with the proton inelastic scattering data to determine the isoscalar structure amplitude. The electron and (p,n) results are tabulated in Table I. For (e,e') the tabulated quantity for each state¹⁴ is

$$\tilde{Z}_i = Z(18.05) \sqrt{F_T(i)/F_T(18.05)},$$

where F_T is the transverse form factor and is explicitly defined in Ref. 14. In the limit that electron scattering were pure isovector, this would give Z_1 . For the (p,n) study, the value of Z_1 is tabulated assuming all states except the 18.2-MeV state were $T=1$. Lebo *et al.*¹⁵ give the fraction of the extreme single-particle sum rule (F_{ESPM}) decomposed by isospin which corresponds to $Z_1^2 / (\sum Z_{1 \text{ ESPM}}^2)$ [see Eq. (6)], i.e., for $T=1$ states $Z_1^2 = F_{\text{ESPM}}/2$. All the (p,n) values of Z_1 have been re-normalized to force $Z_1(18.2)=0.35$ as in the electron scattering work. This increases the (p,n) value by $\sqrt{1.39}$ compared to Ref. 15 (shown later). For most of the $T=1$ states the (e,e') and the (p,n) results are reasonably consistent, particularly when it is remembered that electron scattering is not pure isovector and, as is discussed below, for low-lying stretched states the isovector and isoscalar components are likely to be of opposite phase. An exception is the 11.98-MeV state where the (e,e') and (p,n) are clearly in disagreement. The resolutions of both the 180° (e,e') (150 keV) and (p,n) (370 keV) studies are substantially poorer than that of the (p,p') . The (p,p') spectra, however, are considerably more complex.

The inelastic proton scattering amplitudes, $M_{0(1)}^p$, calculated using the code DW81,¹⁷ are subject to considerable uncertainty. In a comprehensive study of the energy dependence of the excitation of the 6^- states in ^{28}Si , Olmer *et al.*¹⁶ conclude that for several classes of effective nucleon-nucleon interactions, none were able to successfully describe the cross sections and analyzing powers. This suggests that a more reliable procedure would be to make a direct data to data comparison using the measured ^{28}Si angular distributions of the cross sections and analyzing powers and correcting for the slight change in nuclear radius. The ^{26}Mg data provide two excellent test cases for the procedure since one of the excitations (18.05 MeV) is pure $\Delta T=1$ while another (11.98 MeV) is nearly pure $\Delta T=0$.

Excitation of the 18.05-MeV $T=2$ state must be a pure isovector transition. The differential cross section for this state is shown again in Fig. 4 along with the shape (solid curve) determined from the ^{28}Si 14.35-MeV 6^- isovector transition normalized to the experimental data. Similarly in Fig. 5, the analyzing power for this state is exhibited. Also shown as the dashed curves are the results of DWIA calculations. These calculations use the same optical potential as in Ref. 16, again corrected for the slight radius change, a harmonic oscillator parameter for the transi-

TABLE I. Isoscalar and isovector amplitudes for $M6$ excitations in ^{26}Mg . Also shown are spectroscopic factors for single-particle reactions to the same, or to analog states.

E_x (MeV)	T	Z_0	Present work	Z_1	\tilde{Z}^a (e, e')	E_x (p, n)	Z_1^b (p, n)	S^c [$^{25}\text{Mg}(\alpha, ^3\text{He})$]	S^d [$^{25}\text{Mg}(\alpha, t)^{26}\text{Al}$]	S^e [$^{25}\text{Mg}(^3\text{He}, d)$]
9.18	1	-0.14 ± 0.03 (0.20 ± 0.03)		0.15 ± 0.03 (0.30 ± 0.03^f)	0.17	9.3	0.29	0.13	0.20	0.17
11.0										
11.98	1	0.22 ± 0.03		0.04 ± 0.03^g		11.0	0.21		0.08	0.046
12.49	1	0.23 ± 0.04		0.23 ± 0.03	0.19	12.0	0.18	0.029	0.065	0.029
12.83	1	0.26 ± 0.02		0.17 ± 0.02	0.13	12.5	0.25	0.056		0.017
13.00	1				0.11	13.1	0.19	0.013	0.058	0.015
13.97	1				0.12	14.0	0.20	0.005		0.012
14.50	1	0.16 ± 0.02 (-0.04 ± 0.03)	0.17 ± 0.02 (0.16 ± 0.02)		0.15	14.6	0.22	0.017		0.018
15.0						15.0	0.24	0.012		
15.36	1	0.19 ± 0.03		0.18 ± 0.02	0.15	15.5	0.21			0.0095
15.46					0.20					
16.5					0.24	16.5	0.18	0.009		0.012
18.05	2			0.35 ± 0.02^h	0.35		0.35			
		$\sum Z_0^2 = 0.25$ (0.27) ⁱ		$\sum Z_1^2 = 0.29$ (0.36) ⁱ	$\sum \tilde{Z}_1^2 = 0.37$	$\sum Z_1^2 = 0.604$				

^aReference 21.^bReference 21.^cReference 23.^dReference 15, normalized to $Z_1 = 0.35$ for 18.05 MeV; see text.^eReference 14, \tilde{Z} would be Z_1 if (e, e') were pure isovector.^fFrom (p, n), Ref. 23.^gUsing (p, p') angular distribution and absence in (e, e').^hFound to be equal to (e, e') value.ⁱUsing amplitudes for 9.18-MeV state where Z_1 is taken from (p, n).

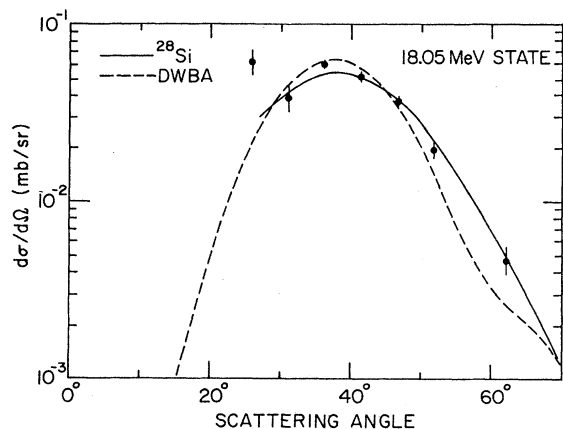


FIG. 4. Differential cross sections for exciting the 18.05-MeV state compared to a $T=1$ excitation in ^{28}Si (solid line) and a DWIA calculation (dashed line).

tion amplitude of $b=1.736$ fm, $\psi \sim \exp[-\frac{1}{2}(r/b)^2]$, and the Franey-Love-85 effective interaction.¹⁸ The agreement of the data-data comparison is excellent, while the DWIA calculation gives a poorer fit to the differential cross sections and significantly underpredicts the analyzing power over most of the angular range.

The (p,p') and (p,n) can also be directly compared for the $T=2$ state. The ratio of the measured cross sections is expected, on isospin considerations, to show $\sigma(p,n)/\sigma(p,p') = \frac{2}{3}$. The extrapolated peak cross sections (at $\theta_{c.m.} \sim 38^\circ$) are in this ratio, although for $\theta_{c.m.} > 40^\circ$, where the data can be directly compared, the angle-averaged ratio is about 0.8. The DWIA analysis of Lebo *et al.*¹⁵ was performed with the same optical potential and residual interaction as the DWIA calculations in the present work, but with a slightly different harmonic oscillator parameter, $b=1.70$. Since only relative (p,n) numbers are tabulated in Table I, the analysis is not sensitive to this difference.

The 6^- state at 11.98 MeV was not observed in the

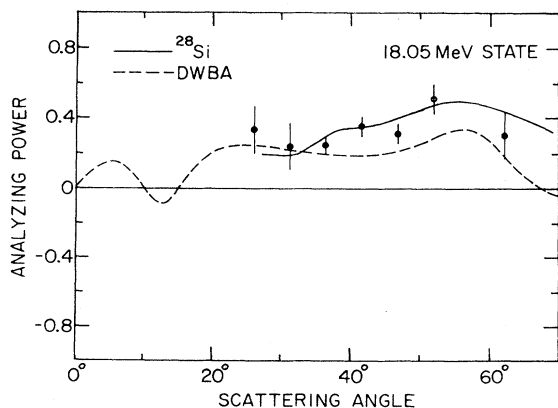


FIG. 5. Analyzing powers for the 18.05-MeV state compared to ^{28}Si (solid line) and a DWIA calculation (dashed line).

electron scattering study. Given the selectivity of 180° (e,e') studies, this implies that the 11.98 state is dominantly an isoscalar excitation in proton scattering and provides a second test case. In Figs. 6 and 7, the angular distributions for the cross sections and analyzing powers for this state are shown relative to the ^{28}Si pattern determined from the 11.58-MeV $T=0$ 6^- state in ^{28}Si and to the DWIA calculation. Again the rescaled data-data comparison is excellent and the DWIA does not successfully reproduce the analyzing powers. In calculating the expected angular distributions and analyzing powers the 3% isovector component needed to make the (e,e') vanish was included with resulting cross sections and analyzing powers that are significantly different from those predicted for a pure isoscalar. The success of the data-data comparisons for these two states establishes that the ^{28}Si data provide reasonable models for M_0^p and M_1^p in ^{26}Mg .

The (p,n) results for the 12.0 state are quite different from the (e,e') results. Given the success of the comparison with ^{28}Si , this suggests that the (p,n) reaction may be populating a $T=0$ state at this excitation energy.

The normalization of the proton amplitudes and the relative phase between M_0^p and M_1^p remain to be determined. The 18.05 MeV state provides an internal calibration for the isovector amplitude relative to electron scattering. There are two sources of confusion in comparing the electron and proton results. The electron scattering amplitudes are calculated in plane wave Born approximation, with Coulomb distortion accounted for by the effective momentum transfer approximation. Traditionally, these results are analyzed including a center of mass correction in momentum space and a correction for two-body or meson exchange currents. The center of mass correction can be included in the coordinate space proton calculation for harmonic oscillator single-particle wave functions by the following: (1) Doing the (p,p') DWIA calculation with an oscillator parameter which is reduced by $\sqrt{(A-1)/A}$ from that

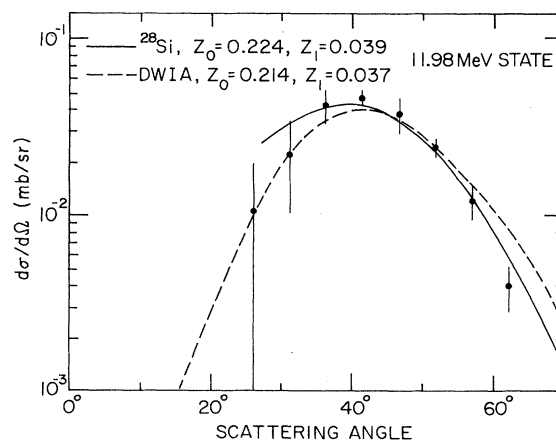


FIG. 6. Fit to the differential cross sections for exciting the 11.98-MeV state using (1) angular distributions measured in ^{28}Si with $Z_0=0.224$, $Z_1=0.039$, (solid line) and (2) a DWIA calculation with $Z_0=0.214$, $Z_1=0.037$ (dashed line).

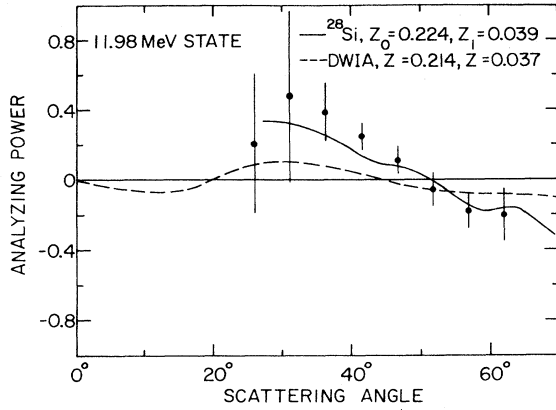


FIG. 7. Comparison of the analyzing powers for the 11.98-MeV state with those predicted using the isospin amplitudes found to best fit the (e, e') and (p, p') differential cross sections (solid line) and DWIA (dashed line).

used in the electron calculations. In Ref. 14, the oscillator parameter $b=1.77$ fm was used. In the present work this is rescaled to 1.736 fm. (2) The calculated (p, p') DWIA cross sections are increased by $[A/(A-1)]^L$ (for 6^- states, $L=5$). The calculated DWIA cross sections in this work include these two center of mass corrections.

Isovector electron scattering also contains contributions from two-body pair and meson exchange currents.¹⁹ Calculations indicate that these increase the calculated form factor for the 18.05 MeV, $T=2$ state by 17% at the peak of the form factor.²⁰ This correction decreases the Z_1^2 needed to fit the experimental cross section by the same factor. A similar fractional increase would be expected for transitions to the $T=1$ states, assuming the electron results for strong states are dominated by isovector interactions. To be consistent, this now implies

$$M_0^e = \frac{(\mu_n + \mu_p)}{\sqrt{1.17(\mu_n - \mu_p)}} M_1^e. \quad (6)$$

Two-body current corrections for proton scattering are less well understood. Arguably, the pair current might be similar in relative magnitude for isovector transitions as in the electron case and negligible for isoscalar transitions. However, given this lack of understanding, the effects of two-body currents have been ignored in analyzing the proton data in the present work.

With these corrections, the electron scattering results determine $Z_1^2=0.122$ for the 18.05-MeV $T=2$ state. The Z_1^2 measured for the ^{28}Si 14.35-MeV $T=1$ state is 0.27. From the ratio of proton cross sections between ^{26}Mg (18.05 MeV) and ^{28}Si (14.35 MeV) a value of $Z_1^2=0.102$ is then obtained for the ^{26}Mg state. The DWIA calculations give a reasonable fit to the ^{26}Mg angular distribution with $Z_1^2=0.094$. We have, in all subsequent calculations rescaled $|M_1^p|^2$ from both the DWIA calculation and the ^{28}Si experiment in order to force Z_1 for the 18.05-MeV state to be the value determined from electron scattering ($Z_1=0.35$).

The ratio of isoscalar to isovector amplitudes

$|M_0^p|/|M_1^p|$ is taken from ^{28}Si also. Here we use the pion inelastic scattering data to determine the ratio Z_0/Z_1 for the ^{28}Si 6^- $T=0$ and $T=1$ states. Since pion inelastic scattering in the $(3,3)$ resonance region is dominated by one s -channel resonance, it is expected that the isospin dependence of the interaction is well understood for high-spin, surface-peaked transitions.³ For this class of transitions, calculated medium modifications are relatively small, in contrast to excitation of low-spin states or quasifree knockout reactions. From the results of Ref. 3 in ^{28}Si , $|M_0^p|/|M_1^p|$ is determined to be 1.55 ± 0.15 at a momentum transfer around 300 MeV/c. We have used this ratio in ^{26}Mg . With the Franey-Love-85 potential,¹⁸ this ratio would be calculated to be 1.37.

It is not possible to determine the phase between M_0^p and M_1^p from the ^{28}Si data and so we must use the DWIA calculations to suggest an appropriate choice. Figure 8 illustrates the relative phase between the isoscalar and isovector amplitudes for the Franey-Love-85 interaction. We have investigated the sensitivity of our results to various choices of phases and find slightly better agreement with the data with the linearly varying phase shown as the solid curve. Our results are not very sensitive to 10° - 20° shifts in the phase or to other similar choices of angular dependence. For example an angle-independent phase of 120° gives comparable results for the fitted structure amplitudes. The DWIA calculations show the phases to vary very little over the excitation energy range of interest and we have therefore used energy independent phases. If the phase, ϕ , were reflected about 90° to $180^\circ - \phi$, the relative sign of the isoscalar and isovector amplitudes would change. This would reverse the relative signs of our fitted Z_0 's and Z_1 's which would interchange proton and neutron states. It would be very important for studies of the reaction mechanism to determine this phase accurately. A comparison of electron, pion, and proton scattering for mixed isospin transitions like those studied here could possibly provide this determination.

For each of the states shown in Figs. 2 and 3, values of

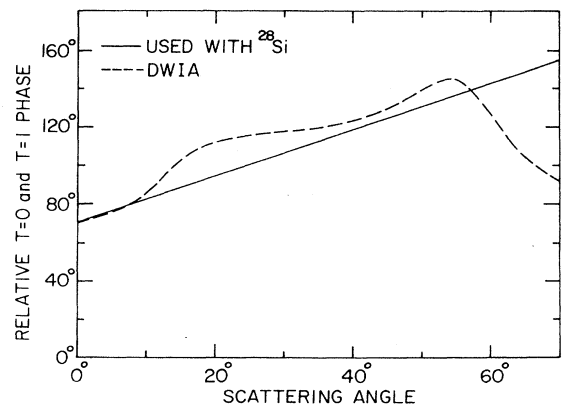


FIG. 8. Phase between the $T=0$ and 1 amplitudes. The dashed line is the phase calculated in the DWIA, while the solid line is the phase used in conjunction with the amplitudes obtained from data taken on ^{28}Si .

Z_0 and Z_1 were determined by the following procedure. The electron scattering angular distributions were consistent with $M6$ transitions and so only one parameter, the form factor at the maximum, was fitted. The electron maximum form factor and the proton differential cross sections were fitted by varying Z_0 and Z_1 . More weight was given to the fit in the region of the maximum of the angular distributions where multistep contributions would be expected to be less important. In general, since Eqs. (1) and (3) are quadratic, two values of Z_0 and Z_1 with opposite relative sign would provide comparable fits and a comparison with the predicted analyzing power could usually distinguish the proper choice. The resulting best fit Z_0 's and Z_1 's are given in Table I. Since only the relative sign is determined, the sign of Z_1 was always chosen to be positive. Figures 9 and 10 show a good example with the 12.49-MeV state. The solid and dashed lines show the two solutions (solid $Z_0=0.231$, $Z_1=0.234$, dashed $Z_0=-0.140$, $Z_1=0.170$). The analyzing powers clearly favor the solid curve. Single values of Z_0 and Z_1 were also determined for the 12.83-MeV state.

For the other states above 13 MeV, the quality of the data is poorer and the fits are less convincing. Based on the proton data alone, it would not be possible to make 6^- assignments to the 14.50, 15.36, and 15.46 and 16.5-MeV states. The 14.50-MeV state is consistent with a 6^- assignment, but the data do not unambiguously distinguish between the two solutions and both are listed in Table I. The electron scattering work reports a group of unresolved states in the region of 16.5 MeV which contain a good bit of 6^- strength, about 50% of that contained in the 18.05 $T=2$ state. No combination of $T=0$ and $T=1$ amplitudes fits both the proton and electron scattering data. The weakness of the state in (p,p') requires $|Z_0| < 0.1$ and $|Z_1| < 0.15$.

The angular distribution for the 15.46-MeV state appears to favor a lower assignment than 6^- . Furthermore, the large negative analyzing power is characteristic of a natural parity state. Based on the present data, it is con-

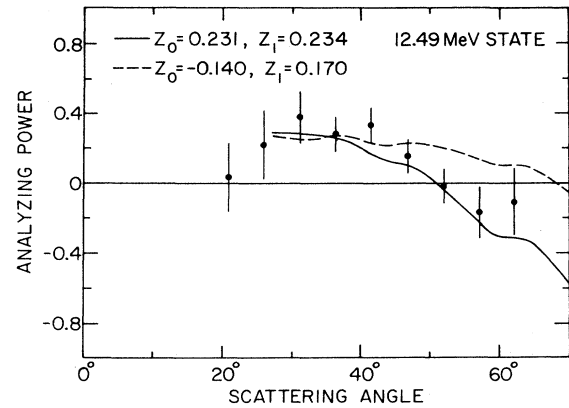


FIG. 10. Measured analyzing powers for the 12.49-MeV state along with those calculated for the two combinations of isospin amplitudes which best fit the angular distribution data (Fig. 9).

cluded that there is little 6^- strength in any state near 15.46 MeV. The fits for the 15.36-MeV state were marginal and are shown in Figs. 11 and 12. A weak state at 7.54 MeV was seen in electron scattering but was not observed in the proton spectra. Fairly weak states reported at 13.00 and 13.97 MeV in (e,e') were not apparent in the (p,p') spectra.

The data for the 9.18-MeV state shown in Figs. 13 and 14 pose the most significant problem. When fitting the proton and electron differential cross sections the solution with $Z_0=-0.137$, $Z_1=0.145$ (solid line in Figs. 13 and 14) gives a good fit to the (p,p') data while the other solution, $Z_0=0.233$, $Z_1=0.209$ (dashed line) does not. The second solution is also not consistent with the analyzing powers while the first solution gives a rather poor, though significantly better, fit. Where $Z_0 \sim -Z_1$ the transition is dominantly a proton excitation since with our isospin convention $Z_0 = -Z_1$ for a pure pro-

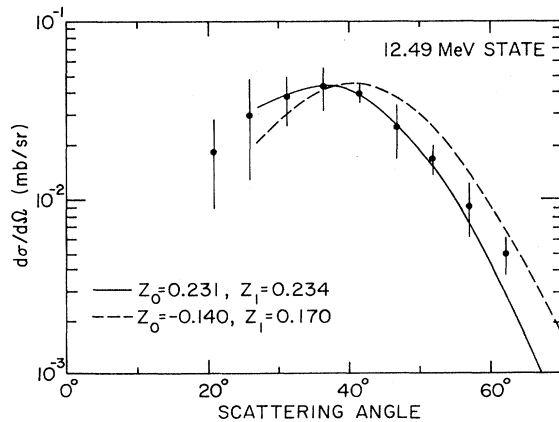


FIG. 9. Angular distribution calculated for the 12.49-MeV state $Z_0=0.231$, $Z_1=0.234$ (solid line) and $Z_0=-0.140$, $Z_1=0.170$ (dashed line) along with the experimental data.

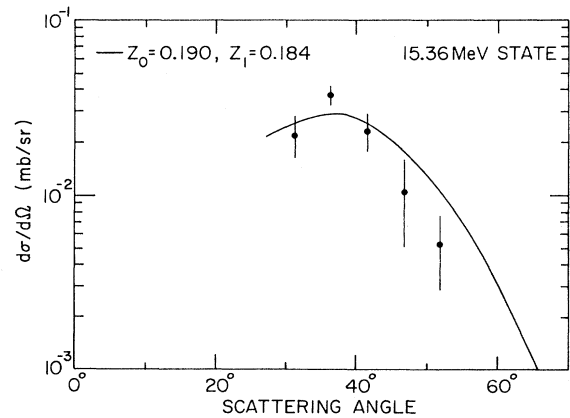


FIG. 11. Calculated and measured angular distribution for the 15.36-MeV state.

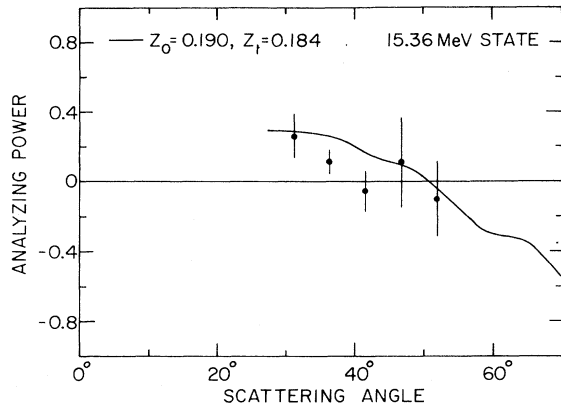


FIG. 12. Calculated and measured analyzing powers for the 15.36-MeV state.

ton transition. Theoretically, this result seems quite unlikely since a proton excitation leaves behind $[(\pi d_{5/2})^3(vd_{5/2})^6]$, which must be $T = \frac{3}{2}$ and therefore several MeV higher than the $T = \frac{1}{2}$ component of the $[(\pi d_{5/2})^4(vd_{5/2})^5]$ remaining after a neutron is elevated. Thus, the lowest-lying $T = 1, 6^-$ states can be expected to be primarily neutron excitations rendering the solution with $Z_0 = -0.137$, $Z_1 = 0.145$ theoretically jarring. It should be noted that the general observation that the analyzing power of the 9.18-MeV state is consistently more positive than that of the 11.98-, 12.49-, and 12.83-MeV states is apparent from the raw spectra, so that attributing this result to an artifact of the fitting procedure seems to be ruled out. The 9.18-MeV state was contained in two momentum settings and the analysis of both gave consistent results.

The more positive analyzing power for the 9.18-MeV

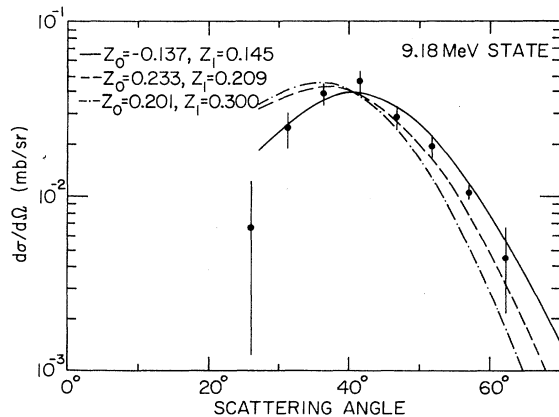


FIG. 13. Fits to the differential cross sections for exciting the 9.18-MeV state. The solid and dashed lines are the two fits that are obtained using the electron scattering data in conjunction with the (p, p') results while the dot-dashed line gives the fit that, in place of the (e, e') data, uses the $Z_1 = 0.30$ obtained in a $^{26}\text{Mg}(p, n)^{26}\text{Al}$ experiment.

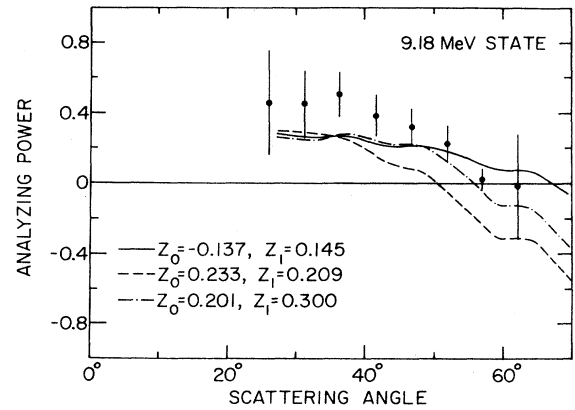


FIG. 14. Analyzing powers for the 9.18-MeV state compared to those predicted using the isospin amplitudes found in fitting the differential cross sections (Fig. 13).

state could be indicative of this state having a larger isovector amplitude than that determined in electron scattering (see Fig. 5). Indeed, the (p, n) work does report a significantly larger value of Z_1 than does the (e, e') . A fit to the (p, n) Z_1 and the (p, p') angular distribution gives the results shown as the dot-dashed curves in Figs. 13 and 14. With the $Z_1 = 0.3$ obtained from the (p, n) reaction the preferred value for Z_0 is 0.20 ± 0.03 . The fit to the differential cross sections is poorer than that obtained using the (e, e') data and the fit to the analyzing powers is not greatly improved. The amplitudes obtained using the (p, n) data for this state are also tabulated in Table I.

It is difficult to reconcile all of the information about the 9.18-MeV state. The (e, e') data is less ambiguous than the (p, n) in that the $^{26}\text{Mg}(p, n)$ reaction can also populate $T = 0$ states in ^{26}Al . However, the fits to the (p, p') data that are obtained when the (e, e') is used in conjunction with the (p, p') are not as good as those obtained for other states. Furthermore, the result that the 6^- state is primarily a proton excitation must be regarded as very surprising. If the (p, n) data is used rather than the (e, e') the overall fits are not better although one does obtain the more theoretically satisfying result of the excitation being primarily neutron. Thus, in regard to the 9.18-MeV state we are left with a puzzle whose solution does not appear to lie in the experimental data.

It must be remembered that \bar{Z}_1 defined above to represent the electron data is not the same as Z_1 . For the majority of states in Table I, the relative sign of Z_0 and Z_1 is positive corresponding to destructive interference between isoscalar and isovector contributions in electron scattering. The Z_1 's obtained from the combined analysis are generally larger than the \bar{Z}_1 's and are in agreement with the Z_1 's obtained from (p, n) for all states where the combined analysis was performed except for the 9.18- and the 11.98-MeV states.

IV. COMPARISON WITH OTHER PROBES

Stretched configuration states can be expected to be strongly excited in single-nucleon transfer reactions

where there is a large momentum mismatch. The 9.18-, 11.98-, 12.49-, 12.85-, and 14.50-MeV states have been found to be populated in the $^{25}\text{Mg}(\alpha, ^3\text{He})^{26}\text{Mg}$ reaction²¹ and their spectroscopic factors are given in Table I. In addition, three other 6^- states are seen very weakly. The total $L=3$ strength seen below 16.5 MeV accounts for a surprisingly small (27.1%) percentage of the sum rule for stripping into the empty $f_{7/2}$ shell. In the $^{25}\text{Mg}(\alpha, t)^{26}\text{Al}$ reaction²² the analogs of the four lowest 6^- $T=1$ states have been seen. Again the sum of the spectroscopic factors is rather small, 40% of the sum rule limit. Most of the $(\alpha, ^3\text{He})$ neutron strength is concentrated in the 9.18-MeV state. This would seem to be inconsistent with the Z coefficients deduced from the proton and electron scattering data, but consistent with the Z coefficients deduced from the proton scattering and charge exchange data. A study of the $^{25}\text{Mg}(^3\text{He}, d)^{26}\text{Al}$ reaction has recently been reported²³ in which the analogs of most of the $T=1$ states that were observed in the present work were populated. In that case only 33% of the sum rule strength was observed with about half of that being in the 9.18-MeV state.

V. DISCUSSION

In the $(d_{5/2}, f_{7/2})$ model for the 0^+ and 6^- states the ground state of ^{26}Mg is $(d_{5/2})^{-2}$ and the excited 6^- states are $[(d_{5/2})^{-3} \times f_{7/2}]_{6^-}$. With this description of the levels there is a sum rule for the nuclear structure amplitudes Z_0 and Z_1 , namely,

$$\sum_i (Z_0^i)^2 = \frac{n_p + n_n}{(4j+2)} = \frac{10}{12}, \quad (6a)$$

$$\sum_i (Z_1^i)^2 = \frac{n_n}{(4j+2)} = \frac{6}{12},$$

for the $T=1$ states,

$$\sum_i (Z_1^i)^2 = \frac{n_p}{(4j+2)} = \frac{4}{12} \quad (6b)$$

for excitation of the 6^- $T=2$ levels, and

$$\sum_i [(Z_0^i)^2 + (Z_1^i)^2] = \frac{n_p + n_n}{2j+1} = \frac{10}{6} \quad (6c)$$

for excitation of all 6^- levels. The quantity $n_p(n_n)$ is the number of protons (neutrons) in the last occupied orbital ($d_{5/2}$). These are generally referred to as the extreme single-particle model sum rules.

From Table I it appears that experimentally the sum of the excitations to $T=1$ levels $\sum_i (Z_0^i)^2 = 0.25$ (0.27) and $\sum_i (Z_1^i)^2 = 0.17$ (0.24), whereas for the $T=2$ state $(Z_1^i)^2 = 0.12$. The numbers in parentheses are those obtained when the (p, n) rather than the (e, e') data are used in determining the amplitudes for the 9.18-MeV state. Thus, the $T=1$ states tabulated in Table I account for only 30% (32%) of the expected isoscalar strength and 33% (47%) of the isovector. For the single $T=2$ level seen in this experiment 37% of the simple sum rule strength has been observed.

Consideration of the nuclear structure in terms of

$(d_{5/2})_0^{-2}$ and $[(d_{5/2})^{-3} f_{7/2}]_{6^-}$ is clearly naive. Generally two classes of nuclear structure effects have been considered for quenching of spin-flip transitions. Several calculations have indicated the importance of $n \geq 2\hbar\omega$ excitations, particularly due to the tensor force.⁷ Certainly, the full (sd) shell is necessary to describe the positive parity levels and the variation of structure through the middle of the (sd) shell. Calculations for ^{28}Si in which the ground state is described by the configuration $(d_{5/2}s_{1/2})_{0^+}^{12}$ and the 6^- levels by $[(d_{5/2}s_{1/2})_{6^-}^{11} f_{7/2}]_{6^-}$ have been carried out.⁵ Calculations on the same basis, $(d_{5/2}s_{1/2})_{0^+}^{10}$ and $[(d_{5/2}s_{1/2})_{6^-}^9 f_{7/2}]_{6^-}$, were done here for ^{26}Mg . Using this configuration space, there are 12 possible 0^+ , $T=1$ states. The shell model Hamiltonian was diagonalized assuming the $(d_{5/2}, s_{1/2})$ interaction of Wildenthal *et al.*²⁴ To diagonalize the shell model Hamiltonian one must know the $(d_{5/2}, f_{7/2})$ and $(s_{1/2}, f_{7/2})$ interaction matrix elements and these were evaluated using the best-fit central spin-dependent potential of Schiffer and True²⁵ with $r_1 = 1.415$ fm and $r_2 = 2.0$ fm. Oscillator functions with $b = 1.847$ fm were used in the calculation of these matrix elements.

If one sums over all the final states, the sum of the cross sections will be proportional to the expectation value of the $d_{5/2}$ number operator, $\sum_m a_{5/2, m}^+ a_{5/2, m}$, evaluated in the ^{26}Mg ground state. In the $(d_{5/2})_{0^+}^{10}$ model there are always 10 particles in the $d_{5/2}$ level. However, in the $(d_{5/2}, s_{1/2})_{0^+}^{10}$ description with the Wildenthal *et al.* interaction²⁴ the expectation value of the $d_{5/2}$ number operator is 8.75. Thus, the sum rule given by Eq. (5) for the Z^2 's decreases from 10/6 to 8.75/6, compared to the experimental value 0.54 (0.63).

The single-particle level spacing between the $d_{5/2}$ and $f_{7/2}$ states is a parameter in the shell model calculation. If this is chosen so that the yrast 6^- , $T=1$ state in the $(d_{5/2}, s_{1/2})_{6^-}^9 f_{7/2}$ calculation is at the observed excitation energy, the yrast $T=2$, 6^- state is predicted at an excitation energy of 18.07 MeV in excellent agreement with the experimental value of 18.05 MeV. The predicted value of Z_1^2 for this state is 0.205 which, although only 61.5% of the $(d_{5/2}, f_{7/2})$ sum rule limit, is 1.7 times that seen experimentally. A second 6^- , $T=2$ state is predicted at about 19.6 MeV and, according to these calculations, has a cross section about a factor of five smaller than that of the 18.05-MeV state. This level has not been in either the (p, p') or the (e, e') studies.

For the $T=1$ states, the yrast 6^- state is predicted to have the spectroscopic strength of $Z_0^2 = 0.088$ and $Z_1^2 = 0.153$ when the $s_{1/2}$ level is included. These numbers are 4.5 (2.2) and 6.8 (1.7) times their experimental counterparts. Except for the 9.18-MeV level, no states are seen or predicted below 11 MeV. Forty $T=1$, 6^- levels are predicted between 11 and 18.05 MeV. Since small changes in the residual two-body interaction can change the individual values of Z_0 and Z_1 for almost degenerate states, it was felt that the best way to compare theory and experiment was to "bin" the values of Z_0^2 and Z_1^2 in 1-MeV intervals. The results of this binning are shown in Fig. 15.

Although much too large a value for Z_0^2 is predicted

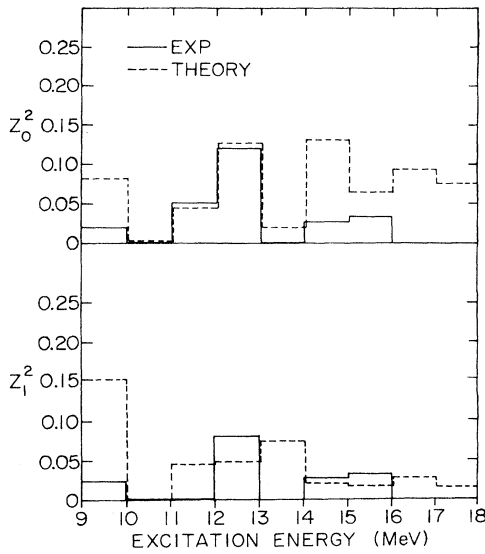


FIG. 15. Comparison of the observed distribution of excitation strength with that calculated in the $(d_{5/2}s_{1/2}f_{7/2})$ model. Upper: isoscalar; lower: isovector. The strengths have been binned in 1-MeV intervals.

for the 9.18-MeV state if the (e, e') rather than the (p, n) data are used, nevertheless, the theoretical values of Z_0^2 follow experiment fairly well up to about 14 MeV. In fact, the predicted sum of Z_0^2 between 9 and 14 MeV is 0.276, whereas experiment gives 0.19 (0.21). Above 14 MeV the calculated Z_0^2 is much larger than seen experimentally. However, very little strength is concentrated in any one state so that even though the sum of the strengths is large, it would be difficult to observe. For example, the strength in the (16–17)-MeV range is slightly larger than the value predicted for the yrast level alone, but the strongest state has a value of Z_0^2 of only $\frac{1}{8}$ that of the 9.18-MeV level. On the other hand, a detailed study of the large predicted strength in the (14–15)-MeV range leads one to the conclusion that more than one 6^- level should have been seen in this region. However, since the $d_{3/2}$ single-particle orbit lies approximately 5 MeV above the $d_{5/2}$, it is precisely in this region that the simple $[(d_{5/2}, s_{1/2})^9 f_{7/2}]$ model should begin to break down. If the calculation using the $[(d_{5/2}, s_{1/2}, d_{3/2})^9 f_{7/2}]$ configuration was performed, then instead of 341 $T=1$, 6^- levels there would be 29 840. Up to 14 MeV the present calculation predicts the sum of Z_1^2 to be 0.32, while, experimentally, only 0.11 (0.17) is found. About half the discrepancy is due to the yrast level.

Considering spectroscopic factors for single-nucleon transfer, the $[(d_{5/2}, s_{1/2})f_{7/2}]$ model gives $S=0.536$ for the yrast 6^- state. This value is about a factor of 3 larger than deduced from the various single-particle transfer reactions^{21–23} (Table I). If the spectroscopic strengths are binned, the model predicts $S=0.116$, 0.157, 0.046, and 0.020 for the strengths in the (11–12)-, (12–13)-, (13–14)-, and (14–15)-MeV regions, respectively. Thus, theory says that 87.5% of the sum rule strength should be seen below

15 MeV, whereas only 27% is seen in the $(\alpha, ^3\text{He})$, 40% in the (α, t) , and 33% in the $(^3\text{He}, d)$ reaction.

While the recently reported single-particle transfer reaction studies to the 6^- states have found spectroscopic factors which are much smaller than the theory predicts, it should be noted that the $^{24}\text{Mg}(\alpha, ^3\text{He})^{25}\text{Mg}$ results, quoted in Ref. 21, for population of the $\frac{7}{2}^-$ level lead to a value of S which is a factor of 2–3 smaller than seen in the (d, p) reaction²⁶ and in an earlier $(\alpha, ^3\text{He})$ experiment.²⁷ The predicted ratio

$$\frac{Z_N^2}{S_N} = \left[\frac{Z_0 + Z_1}{\sqrt{2}} \right]^2 \frac{1}{S_N} \quad (7)$$

of the neutron inelastic scattering strength to the neutron stripping spectroscopic factor varies by a factor of 2 from state to state for the strong states, as do the experimental ratios. Such behavior is indicative of the existence of significant interference between the various terms in the sum of Eq. (4). A major problem with the ^{28}Si calculation⁵ was that the predicted Z_p^2/S_p ratio was similar for the various ^{28}Si 6^- states, in disagreement with experiment. For ^{26}Mg , the theory and experiment agree in general for inelastic scattering except for the values of Z_0 and Z_1 predicted for excitation of the yrast 6^- $T=1$ state.

Particularly for Z_0^2 , a large amount of strength is predicted above 14-MeV excitation, ($\sum Z_0^2=0.363$ from 14 to 18 MeV), whereas $\sum Z_0^2=0.062$ for the two observed states. However, not only is the theoretical strength spread over many levels in the $[(d_{5/2}, s_{1/2})f_{7/2}]$ model, thereby making observation difficult, but this is exactly where contributions from the $d_{3/2}$ orbit are likely to become important and cause additional dilution of the strength. Consequently, it is not surprising that a large amount of the Z_0 strength has been missed.

Recently Clausen *et al.*²⁸ have calculated isovector electron scattering to stretched states and have shown that the extracted amplitude can be significantly different when Woods-Saxon, rather than bound, harmonic oscillator wave functions are used. Given the problems associated with the t matrix for proton inelastic scattering discussion in Sec. III, it would be difficult to incorporate this state-dependent effect into the present analysis.

VI. CONCLUSIONS

In summary, the present work has demonstrated that a combination of electron scattering, polarized proton scattering, and proton charge exchange data can be used to extract isospin amplitudes for the excitation of high-spin stretched configuration states. The specific assumptions required are the following: (1) The shape of the angular distributions for spin-up and spin-down proton inelastic scattering to states of given isospin can be determined in a neighboring nucleus, ^{28}Si . The spin-dependent cross sections are not adequately reproduced by DWIA calculations. (2) The normalization of the isovector amplitude can be determined by comparison with electron scattering for a pure isovector transition. (3) The relative normalization of the isoscalar and isovector amplitudes

TABLE II. Ratio of total observed inelastic scattering strength to that predicted by the minimum configuration model for "stretched" excited states [Eq. (5)]. T_0 is the isospin of the ground state.

Nucleus	J_{ex}^{π}	$T = T_0$		$T = T_0 + 1$	All $\Delta T = 1$	Ref.
		$\Delta T = 0$	$\Delta T = 1$	$\Delta T = 1$		
^{14}N	5^-	0.35		0.60	0.60	11
^{16}O	4^-	0.23		0.41 (0.52)	0.41 (0.52)	12
^{24}Mg	6^-	<0.11		0.27	0.40	2
^{26}Mg	6^-	0.32 (0.32)	0.33 (0.47)	0.37	0.35 (0.43)	Present work
^{28}Si	6^-	0.14		0.37	0.37	3
^{54}Fe	8^-	0.11	0.29	0.52	0.38	4

can be determined in ^{28}Si by a comparison of proton and pion scattering. If this relative normalization would have been determined by DWIA calculations with the Franey-Love-85 interaction,¹⁸ the results would have changed by less than 20%. (4) The relative phases of the isoscalar and isovector amplitudes are close to those given by the DWIA with the Franey-Love-85 interaction.

The isospin amplitudes are well determined for the 11.98-, 12.49-, and 12.83-MeV states. The 11.98-MeV state appears to be an isoscalar excitation, which would imply that the state observed in (p, n) at 12.0 MeV is a $T=0$ state. The analysis is much less certain for the 14.50- and 15.36-MeV states.

A fit to the 9.18 state resulted in an unreasonable proton structure for this state using the (e, e') results. With the (p, n) value of Z_1 , the fit to the differential cross sections was not as good but the structure for this state was then similar to that predicted by a shell model calculation as well as to that determined for the yrast stretched state⁴ in ^{54}Fe .

Inelastic scattering strengths that have been reported in various nuclei are tabulated in Table II, where it can be seen that the summed isovector strength observed in ^{26}Mg is similar to that observed in neighboring nuclei. Substantially more isoscalar strength is identified in ^{26}Mg

than in ^{28}Si or ^{24}Mg . This rapid variation is not understood. Perhaps it is related to the rapid variation of deformation through the s - d shell. The importance of deformation in the quenching of high-spin transitions has been discussed by Liu and Zamick.²⁹ The shell model calculations are more successful in reproducing the ^{26}Mg results than in ^{28}Si . However, this may merely reflect the fact that more 6^- strength is identified in ^{26}Mg .

It is clear that given the lack of a selective probe for isoscalar spin flip excitations, the type of isospin decomposition described here or performed with pion inelastic scattering data⁴ will be required to study this mode of the nuclear excitation. The DWIA calculations suggest that the proton spin-flip probability may provide a much more sensitive tool for isospin decomposition. Such a new tool would be extremely welcome.

ACKNOWLEDGMENTS

The authors wish to thank B. D. Anderson for making available the (p, n) data prior to publication. This work supported in part by the U.S. Department of Energy, Nuclear Physics Division, under Contract W-31-109-ENG-38, and by the National Science Foundation.

*Permanent address.

†Permanent address: Obafemi Awolowo University, Ile-Ife, Nigeria.

¹F. Petrovich, J. A. Carr, and H. McManus, *Annu. Rev. Nucl. Part. Sci.* **36**, 29 (1986).

²G. S. Adams, A. D. Bacher, G. T. Emery, W. P. Jones, R. J. Kouzes, D. W. Miller, A. Picklesimer, and G. E. Walker, *Phys. Rev. Lett.* **38**, 1387 (1977).

³C. Olmer, B. Zeidman, D. F. Geesaman, T.-S. H. Lee, R. E. Segel, L. W. Swenson, R. L. Boudrie, G. S. Blanpied, H. A. Thiessen, C. L. Morris, and R. E. Anderson, *Phys. Rev. Lett.* **43**, 612 (1979).

⁴D. F. Geesaman, R. D. Lawson, B. Zeidman, G. C. Morrison, A. D. Bacher, C. Olmer, G. R. Burleson, W. B. Cottingham, S. J. Greene, R. L. Boudrie, C. L. Morris, R. A. Lindgren, W. H. Kelly, R. E. Segel, and L. W. Swenson, *Phys. Rev. C* **30**, 952 (1984).

⁵A. Amusa and R. D. Lawson, *Phys. Rev. Lett.* **51**, 103 (1983).

⁶S. Krewald and J. Speth, *Phys. Rev. Lett.* **45**, 417 (1980).

⁷A. Shimizu, M. Ichimura, and A. Arima, *Nucl. Phys.* **A226**, 282 (1974).

⁸W. Knüpfner, M. Dillig, and A. Richter, *Phys. Lett.* **95B**, 349 (1980).

⁹E. Oset and M. Rho, *Phys. Rev. Lett.* **42**, 47 (1979).

¹⁰C. L. Morris, J. Piffaretti, H. A. Thiessen, W. B. Cottingham, W. J. Braithwaite, R. J. Joseph, I. B. Moore, D. B. Holtkamp, C. J. Harvey, S. J. Greene, C. F. Moore, R. L. Boudrie, and R. J. Peterson, *Phys. Lett.* **86B**, 31 (1979).

¹¹J. C. Bergstrom, R. Neuhausen, and G. Lahm, *Phys. Rev. C* **29**, 1168 (1984).

¹²J. A. Carr, F. Petrovich, D. Halderson, D. B. Holtkamp, and W. B. Cottingham, *Phys. Rev. C* **27**, 1636 (1983); C. E. Hyde-Wright, W. Bertozzi, T. N. Boti, J. M. Finn, F. W. Hersman, M. V. Hynes, M. A. Kovash, J. J. Kelly, S. Kowalski, J. Lichtenstadt, R. W. Lourie, B. E. Norman, B. Pugh, C. P. Sargent, B. L. Berman, F. Petrovich, and J. A. Carr, *Phys. Rev. C* **35**, 880 (1987).

¹³W. L. Blendel, L. W. Fagg, R. A. Tobin, and H. F. Kaiser,

- Phys. Rev. **173**, 1103 (1968).
- ¹⁴M. A. Plum, R. A. Lindgren, R. S. Hicks, R. L. Huffman, G. A. Peterson, P. R. Ryan, L. D. Phan, X. K. Maruyama, C. Olmer, A. D. Bacher, and D. F. Geesaman (unpublished); M. A. Plum, Ph.D. thesis, University of Massachusetts, 1985 (unpublished).
- ¹⁵C. Lebo, B. D. Anderson, T. Chittakon, A. R. Baldwin, R. Madey, J. W. Watson, and C. C. Foster, Phys. Rev. C **38**, 1099 (1988).
- ¹⁶C. Olmer, A. D. Bacher, G. T. Emery, W. P. Jones, D. W. Miller, H. Nann, P. Schwandt, S. Yen, T. E. Drake, and R. J. Sobie, Phys. Rev. C **29**, 361 (1984).
- ¹⁷Program DWBA70 by R. Schaeffer and J. Raynal (unpublished); extended by J. R. Comford (unpublished code DW81).
- ¹⁸M. A. Franey and W. G. Love, Phys. Rev. C **31**, 488 (1985).
- ¹⁹S. Krewald, A. M. Lallena, and J. S. Dehesa, Nucl. Phys. **A448**, 685 (1986), and references therein.
- ²⁰R. A. Lindgren, M. Leuschner, B. L. Clausen, R. J. Peterson, M. A. Plum, and F. Petrovich, in *Nuclear Structure at High Spin, Excitation, and Momentum Transfer (Indiana, 1985)*, Proceedings of the Conference on Nuclear Structure at High Spin, Excitation, and Momentum Transfer, AIP Conf. Proc. No. 142, edited by H. Nann (AIP, New York, 1986), p. 133.
- ²¹J. J. Kraushaar, M. Fujiwara, K. Hosono, H. Ito, M. Kondo, H. Sakai, M. Tosaki, M. Yasue, S. I. Hayakawa, and R. J. Peterson, Phys. Rev. C **34**, 1530 (1986).
- ²²R. J. Peterson, B. L. Clausen, J. J. Kraushaar, H. Nann, W. W. Jacobs, R. A. Lindgren, and M. A. Plum, Phys. Rev. C **33**, 31 (1986).
- ²³R. J. Peterson, M. Yasue, M. H. Tanaka, T. Hasegawa, N. Nisimura, H. Ohnuma, H. Shimizu, K. Ieki, H. Toyokawa, M. Iwase, J. Iimura, and S. I. Hayakawa, Phys. Rev. C **38**, 1130 (1988).
- ²⁴B. H. Wildenthal, J. B. McGrory, E. C. Halbert, and P. W. M. Glaudemans, Phys. Lett. **26B**, 692 (1968).
- ²⁵J. P. Schiffer and W. W. True, Rev. Mod. Phys. **48**, 191 (1976).
- ²⁶F. Neuders and G. de Korte, Nucl. Phys. **A249**, 205 (1975).
- ²⁷G. C. Yang and P. P. Singh, Proc. Amsterdam Conf. **1**, 183 (1974).
- ²⁸B. L. Clausen, R. J. Peterson, and R. A. Lindgren, Phys. Rev. C **38**, 589 (1988).
- ²⁹H. Liu and L. Zamick, Phys. Rev. C **32**, 1754 (1985).